COMMUNICATION

Low Temperature Insights into the Crystal and Magnetic Structure of a Neutral Radical Ferromagnet

Received 00th January 20xx,
Accepted 00th January 20xx

DOI: 10.1039/x0xx00000x

Craig M. Robertson,*[a] Stephen M. Winter,[b] Judith A. K. Howard,[c] Michael R. Probert[d] and Richard T. Oakley*[e]

The crystal structure of the radical ferromagnet 1a at 2 K reveals a contraction in the unit cell *c* constant which, at the molecular level, translates into a decrease in slippage of the radical π-stacks and an increase in ferromagnetic exchange interactions along the stacking axis. The results of BS-DFT calculations using long-range corrected functionals are consistent with an overall ferromagnetic topology.

The development of non-metal based magnetic materials using neutral organic radicals (S = ½) as building blocks has revealed appealing conceptual links between the behavior of unpaired electrons in p-, d- and f-orbitals.[1] In postulating the origins of ferromagnetism in 1928, Heisenberg asserted that magnetic exchange energies sufficiently large to overcome thermal energies (>kT) require the presence of spin density on heavy atoms, that is, with principal quantum number PQN ≥ 3.[2] Consistently, the ordering (Curie) temperatures T_C of the first p-block radical ferromagnets, all built from light atoms (PQN < 3), were less than 2 K.[3] Moreover, in the absence of appreciable magnetic anisotropy, coercive fields H_c were vanishingly small.[4] However, by incorporating heavier elements, i.e., sulfur (PQN = 3) into spin-bearing sites, magnetic order at higher temperatures proved possible,[5] although H_c values remained low (< 10 Oe).

Introduction of selenium (PQN = 4) led to enhancements in both isotropic and anisotropic exchange energies. In the case of resonance stabilized bisdiselenazolyl radicals **1** (Fig. 1),[6] the structural diversity afforded by different R_1/R_2 combinations yielded a range of magnetic phases,[7,8] including the ferromagnets **1a**,**b**,**c** (R_1 = Et; R_2 = Cl, Br, I),[9] which crystallize in the tetragonal space group $P\bar{4}2_1m$ and display not only high ordering

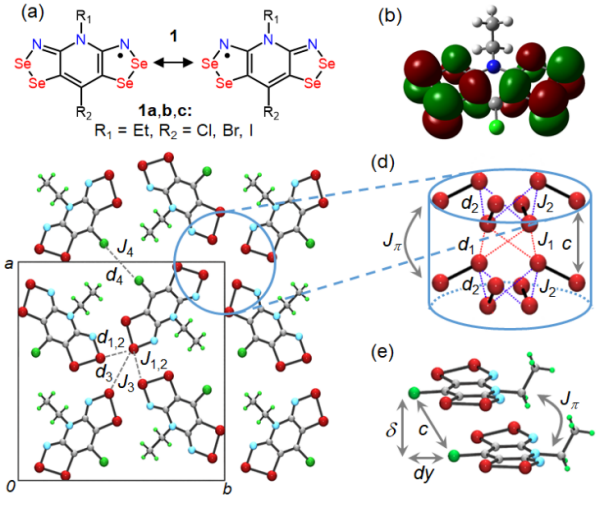

Fig. 1 (a) Bisdiselenazolyl radicals **1a**,**b**,**c**. (b) Kohn-Sham SOMO for **1a**. (c) Pinwheel packing of radical π-stacks in **1a**, with intermolecular contacts d_1-d_4 and associated exchange energies J_1-J_4; (d) Alternation of $d_{1,2}$ ($J_{1,2}$) along π-stacks. (e) Intrastack plate (mean plane) separation δ, π-stack slippage dy and exchange energy J_π.

temperatures T_C = 17 K, 17.5 K and 10.5 K, but also large coercive fields H_c = 1370, 1600 and 370 Oe at 2 K.

High field EPR studies[10] on **1a** established the presence of easy-axis magnetic anisotropy, with the crystallographic *c*-axis (the π-stacking direction) as the easy axis and the *ab* plane as the hard plane. The magnitude of anisotropic exchange interactions and H_c arise from spin-orbit coupling occasioned by the presence of selenium, while the value of T_C depends largely on isotropic exchange interactions. Attempts to quantify the latter have posed a challenge. Broken symmetry density functional theory BS-DFT methods have been used extensively to estimate magnetic exchange energies in light-atom radicals,[11,12] and even in heavy-atom radicals afford qualitative insights,[8] but a more detailed grasp of the magnitude of isotropic exchange interactions in **1a** has not, to date, been achieved. In light of the known effects of temperature-induced structural changes on exchange energies,[13] securing precise information on the structure of **1a** in its ordered state constitutes a vital first step.

[a] *Department of Chemistry, University of Liverpool, Liverpool L69 7ZD, UK.*
[b] *Department of Physics, Wake Forest University, Winston-Salem, NC 27109, USA.*
[c] *Department of Chemistry, Durham University, Durham, DH1 3LE, UK.*
[d] *Chemistry, School of Natural and Environmental Sciences, Newcastle University, Newcastle upon Tyne, NE1 7RU, UK.*
[e] *Department of Chemistry, University of Waterloo, Waterloo, Ontario N2L 3G1, Canada.*

† Electronic supplementary information (ESI) available: Details of crystallographic work and theoretical calculations. CCDC 2096260. For ESI and crystallographic data in CIF format see DOI: 10.1039/x0xx00000x

Table 1 Structural Parameters for **1a**.[a]

T (K)	296(2) [b]	100(2) [b]	2(1)
a, b (Å)	16.2708(5)	16.1801(12)	16.1915(4)
c (Å)	4.1720(3)	4.1264(6)	4.07570(10)
V (Å^3)	1104.49(9)	1080.27(8)	1068.50(6)
d_1 (Å)	3.404(1)	3.357(1)	3.2420(6)
d_2 (Å)	3.502(1)	3.457(1)	3.4404(6)
d_3 (Å)	3.8907(9)	3.8324(9)	3.8322(5)
d_4 (Å)	3.967(3)	3.893(3)	3.861(1)
δ (Å)	3.567(6)	3.511(4)	3.485(1)
dy (Å)	2.164(6)	2.168(7)	2.113(1)

[a] See Fig. 1 for definition of contacts. [b] From reference 9a.

We have therefore determined the crystal structure of radical **1a** at 2 K,[14] well below its FM ordering temperature of 17 K. Unit cell parameters are presented in Table 1, along with those obtained previously at 296 K and 100 K.[9a] The results confirm that the space group $P\bar{4}2_1m$ remains unchanged. As expected, there is a steady contraction in the cell volume V with cooling, driven mainly by a decrease in the cell c constant. However, while the value of the cell a,b constants also decrease between 296 K and 100 K, they actually *increase* on cooling to 2 K.

At the molecular level the contractions observed in the internal bonds are nominal. More important are the changes in the intermolecular contacts defined in Figure 1. The two lateral Se···Se′ contacts d_1 and d_2 alternate along the z-direction, lacing together out-of-register radicals in adjacent π-stacks. These contacts, which are well within the expected van der Waals (VDW) separation,[15] define the pairwise exchange energies J_1 and J_2. There is a third Se···Se′ contact d_3 linking radicals into chains running along glide planes, and also a localized Cl···Cl′ contact d_4. Both d_3 and d_4 lie near or outside the respective VDW separation,[15] but the related exchange energies J_3 and J_4 are considered here for completeness. The final but most important contact is the interplanar separation δ between neighboring radicals along the π-stacks; as expected its value contracts steadily over the entire temperature range. The corresponding exchange energy J_π proves to be very sensitive to temperature, in part because of the contraction in δ itself, but also because of changes in the cell c constant and hence the π-stack slippage parameter dy, which rises slightly between 296 K (2.164(6) Å) and 100 K (2.168(7) Å), but decreases significantly (to 2.113(1) Å) on further cooling to 2 K. The magnetic consequences of this seemingly minor adjustment are profound.

Ferromagnetic order and the value of T_C observed in **1a** is determined by the magnitude and sign of the individual intermolecular magnetic interactions which, in the absence of spin-orbit effects, may be defined in terms of the isotropic Heisenberg Hamiltonian $H_{ex} = -2J_{ij}\{S_i \cdot S_j\}$. In this convention $J_{ij} > 0$ corresponds to a preference for FM alignment of spins on adjacent sites, while $J_{ij} < 0$ denotes an AFM preference. From a theoretical perspective these interactions are often described in terms of the two-site single orbital Hubbard model,[16] in which

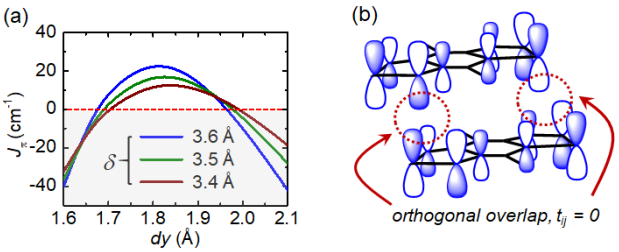

Fig. 2 (a) UB3LYP/6-31G(d,p) J_π values for model radical **1** ($R_1 = R_2 = H$) as a function of π-stack slippage dy at different plate separations δ. (b) The orthogonal overlap condition ($t_{ij} = 0$) for SOMOs on adjacent radicals along the π-stacks.

the isotropic exchange energy J_{ij} between neighboring pairs (i,j) of radicals is expressed as in eq. 1.

$$2J_{ij} = 2K_{ij} - 4(t_{ij})^2/U \qquad \text{(eq. 1)}$$

In this equation U is the onsite Coulomb potential, t_{ij} the intermolecular hopping (or resonance) integral for interactions between neighboring singly occupied molecular orbitals (for a single SOMO, see Fig. 1b) and K_{ij} the electron exchange integral, the source of Hund's coupling. Qualitatively, strong overlap leads to a large virtual hopping term $4(t_{ij})^2/U$ which favors antiferromagnetic (AFM) exchange (–ve J), while FM exchange (+ve J) is preferred when SOMO-SOMO overlap is orthogonal and t_{ij} nullified.[17] In most cases the magnitude of J_{ij} is set by the virtual hopping term. However, with the inclusion of intersite electron exchange, which is generally small but always +ve, the balance may be shifted in favor of a net FM interaction, as in the present case.

Of the five intermolecular interactions identified in Fig. 1, two (d_3, d_4) are close to or beyond the nominal VDW separation; both hopping (t_{ij}), exchange (K_{ij}) integrals and the resulting exchange energies J_3, J_4 are likely to be small. The source of the ferromagnetic order must therefore stem from FM (+ve) values for J_1, J_2 and J_π. In the BS-DFT approximation,[18] the exchange energy J_{ij} between two radicals is estimated from the total energies of the triplet (E_{TS}) and broken symmetry singlet (E_{BSS}) states and the respective expectation values $< S^2 >$, as in eq. 2.

$$J = -\frac{(E_{TS} - E_{BSS})}{< S^2 >_{TS} - < S^2 >_{BSS}} \qquad \text{(eq. 2)}$$

In the $P\bar{4}2_1m$ space group of **1a**,**b**,**c** the radicals are bisected by a mirror plane which confines slippage of radicals within the π-stacks to the single variable dy. Values of J_π calculated as a function of this coordinate for model structures with different radical separations δ (Fig. 2a) indicate that axial exchange is strongly AFM (–ve) save for in the narrow range $dy \sim 1.7 - 2.0$ Å, where it rises briefly into FM (+ve) territory. This result finds a satisfying explanation in terms of the Hubbard model (eq.1), as it is precisely in this region where the SOMO-SOMO overlap between adjacent radicals (Fig. 2b) becomes orthogonal and the virtual hopping term vanishes. From a design perspective, the implications are profound. Only structures with a π-stack displacement within this narrow range of dy will display a ferromagnetic J_π, without which there can be no FM ordering, regardless of the values of J_1 and J_2. Even small variations in dy

can have large magnetic consequences.[19] Thus, despite the overall structural similarity of **1a**,**b**,**c**, the interplanar spacing δ and π-stack slippage *dy* for **1c** are fractionally larger than found in **1a**,**b**, sufficiently so to reduce the value of T_C.[9c] On the plus side, the pressure-induced increase in T_C for all three radicals can be readily appreciated in terms of the concomitant decrease in both δ and *dy*, which causes a sharp rise in J_π.[9c,20]

Despite these qualitative successes, reproducing accurately the full 3D magnetic topology of **1a**,**b**,**c** by BS-DFT methods has remained a challenge. Part of the problem, at least in the case of **1a**, stems from the subtle temperature-driven change in π-stack slippage revealed in the 2K structure. Calculated exchange energies, for J_π in particular, based on the use of even the 100 K coordinates, do not adequately reflect those found at the ordering temperature T_C. In addition, limitations in the computational method itself probably play a part; DFT functionals affording a better balance between electron exchange and virtual hopping parameters (eq. 1) are needed.

To address both these points we have performed a series of BS-DFT calculations of the five pairwise exchange interactions $J_{1\text{-}4}$ and J_π found in **1a**, using coordinates for radical pairs taken from the data sets collected at 296 K, 100 K *and* 2 K. We explored a range of functionals with the most commonly employed hybrid functional B3LYP[21] serving as a benchmark; the triple-ξ quality 6-311G(d,p) basis set was employed in all cases. Values for the dominant contributors J_1, J_2 and J_π are listed in Table 2 and presented in histogram form in Fig. 3; a complete listing of all *J*-values (including J_3, J_4) is provided in Table S2. Also shown in Table 2 are theoretical estimates of the Θ-constant derived using the mean-field approximation defined in eq. 3,[22] where *zJ* is the sum of the near-neighbor pairwise exchange interactions identified in Fig. 1 (see also Fig. S1).

$$zJ = \frac{3k_B\Theta}{2S(S+1)} \qquad \text{(eq. 3)}$$

The B3LYP calculated *J*-values show little change with temperature between 296 K and 100 K, with J_1 being consistently much larger than J_2. Of greater concern is the strongly –ve (AFM) value for J_π, which becomes slightly more AFM on cooling from 296 K to 100 K. However, with a further decrease in temperature to 2 K, J_π becomes significantly less –ve, while J_1 and J_2 remain relatively constant. Overall, however, B3LYP fails to capture the essence of the magnetic structure, that is, the requirement that all three exchange interactions be +ve in order to achieve bulk ferromagnetic order.

In considering other functionals,[23] we focused on those which treat Hartree-Fock (HF) exchange more aggressively. As a first step we selected the related hybrid PBE0 functional,[24] which employs a slightly greater contribution (25% HF) compared to B3LYP (20% HF). The results reveal a marginal improvement, a less –ve J_π value at 296 K which actually turns +ve at 2 K, but still with a consistently near zero value for J_2. At this point we considered more general problems that can afflict standard hybrid functionals such as B3LYP and PBE0, in particular the fact that the non-Coulomb part of the functional is known to decay too rapidly, becoming inaccurate at large distances, thereby making the functional less effective for energies involving electron excitations to higher orbitals.

Table 1 BS-DFT Exchange Energies for **1a**.[a,b]

	T (K)	J_1 (cm^{-1})	J_2 (cm^{-1})	J_π(cm^{-1})	Θ (K) [c]
B3LYP	296	4.92	0.13	-6.97	3.5
	100	5.64	0.15	-7.75	4.5
	2	5.55	-0.29	-1.57	11.6
PBE0	296	5.14	0.83	-4.11	10.5
	100	5.86	0.94	-4.59	12.3
	2	5.77	0.55	1.16	18.9
CAM-B3LYP	296	2.90	1.32	1.23	13.3
	100	3.36	1.45	1.40	15.2
	2	3.34	1.29	5.54	20.5
ωB97XD	296	3.16	1.56	2.27	16.3
	100	3.56	2.04	3.35	20.4
	2	3.51	2.06	5.87	23.7
LC-ωHPBE	296	2.15	1.29	4.49	15.9
	100	2.50	1.47	5.13	18.4
	2	2.48	1.36	8.77	23.1

[a] 6-311G(d,p) basis set. [b] For J_3, J_4 values, see Table S2. [c] Estimated from the mean-field approximation (eq. 3) as $\Theta = 0.5\ zJ/k_B$, where $zJ = 4J_1 + 4J_2 + 2J_3 + J_4 + 2J_\pi$.

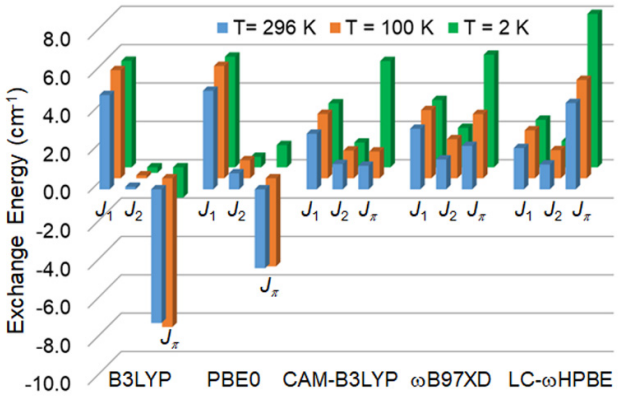

Fig. 3 Histogram of BS-DFT exchanges energies J_1, J_2 and J_π (in cm^{-1}) for **1a**, using different functionals and structural data collected at 296 K, 100 K and 2 K.

Long-range corrected (LC) functionals, in which the degree of HF exchange is enhanced at greater distances, were developed in part to address this problem.[25] To test the possibility that they might also function well at modelling exchange energies for long range interactions in **1a**, we selected CAM-B3LYP (65% long range HF),[26] ωB97XD[27] and LC-ωHPBE (each 100% long range HF)[28] and recalculated the exchange energies for **1a**. The results were encouraging; all three afford +ve (FM) values for the axial exchange energy J_π, even when using the 296 K structural data. Moreover, its value increases markedly between 100 K and 2 K, almost doubling for ωB97XD and LC-ωHPBE and more than trebling for CAM-B3LYP. The latter still affords the smallest J_π value at 2 K, a result which may reflect the fact that it employs a lower proportion of HF exchange in the long range region.[29]

In contrast to the marked temperature dependence of J_π, the response of the lateral exchange couplings J_1 and J_2 to temperature is relatively small, a result consistent with the small observed changes in d_1 and d_2 with temperature. We also note

that the mean-field estimates for the Θ-constant obtained from the 2 K coordinates using all three LC-functionals are broadly consistent with the Curie-Weiss value of 22.9 K.[9a]

While a full understanding of the behavior of heavy-atom radical magnets requires the explicit inclusion of spin-orbit effects in the magnetic Hamiltonian, the present results on **1a** provide insight into the sign and magnitude of isotropic exchange interactions and their role in defining the onset of magnetic order. All three LC functionals reveal an increasing 1D topology from 296 K down to 2 K. While the lateral exchange interactions J_1 and J_2 remain relatively constant with decrease in temperature, the axial interaction J_π increases substantially, especially below 100 K, where temperature driven adjustments in the degree of slippage of the π-stacks are greatest. In light of these results it is intriguing to consider whether similar structural and magnetic adjustments may be found at low temperature in other heavy-atom radicals.

Despite their improved performance we do not view the use of LC functionals as a panacea; there is clearly room for continued exploration of other functionals and indeed other theoretical approaches[30,31] for the study of radical-based magnetic materials, especially multi-orbital systems,[1,32] where the presence of low-lying virtual orbitals promotes FM exchange. Regardless of the choice of method, however, the present results demonstrate the critical need for collecting structural information at temperatures near or below the transition to a magnetically ordered state.[32,33] Such data represents an essential prerequisite for the realistic assessment of isotropic exchange energies within the magnetically ordered regime.

We acknowledge the following for financial support: NSERC of Canada (to CMR and RTO), WFU Center for Functional Materials (to SMW) and EPSRC (to JAKH and MRP). We thank the late Dr. Andrés Goeta for helpful discussions.

Notes and references

[1] S. M. Winter, S. Hill and R. T. Oakley, *J. Am. Chem. Soc.,* 2015, **137**, 3720.
[2] W. Heisenberg, *Z. Phys.,* 1928, **49**, 619.
[3] (a) M. Tamura, Y. Nakazawa, D. Shiomi, K. Nozawa, Y. Hosokoshi, M. Ishikawa, M. Takahashi, M. Kinoshita, *Chem. Phys. Lett*., 1991, **186**, 401. (b) R. Chiarelli, M. A. Novak, A. Rassat, J. L. Tholence, *Nature,* 1993, **363**, 147.
[4] P. Day, *Nature*, 1993, **363**, 113.
[5] (a) A. J. Banister, N. Bricklebank, I. Lavender, J. M. Rawson, C. I. Gregory, B. K. Tanner, W. Clegg, M. R. J. Elsegood, F. Palacio, *Angew. Chem., Int. Ed. Engl.*, **1996**, 35, 2533; (b) W. Fujita, K. Awaga, Y. Nakazawa, K. Saito and M. Sorai, *Chem. Phys. Lett*., 2002, **352**, 348; (c) R. I. Thomson, C. M. Pask, G. O. Lloyd, M. Mito and J. M. Rawson, *Chem. Euro. J*., 2012, **18**, 8629.
[6] Y. M.Volkova, A. Y. Makarov, E. A. Pritchin, N. P. Gritsan and A. V. Zibarev, *Mendeleev Commun*., 2020, **30**, 385.
[7] A. A. Leitch, J. L. Brusso, K. Cvrkalj, R. W. Reed, C. M. Robertson, P. A. Dube and R. T. Oakley, *Chem. Commun*., 2007, 3368.
[8] A. A. Leitch, X. Yu, S. M. Winter, R. A. Secco, P. A. Dube and R. T. Oakley, *J. Am. Chem. Soc*., 2009, **131**, 7112.
[9] (a) C. M. Robertson, A. A. Leitch, K. Cvrkalj, R. W. Reed, D. J. T. Myles, P. A. Dube and R. T. Oakley, *J. Am. Chem. Soc.*, 2008, **130**, 8414; (b) A. A. Leitch, K. Lekin, S. M. Winter, L. E. Downie, H. Tsuruda, J. S. Tse, M. Mito, S. Desgreniers, P. A. Dube, S. Zhang, Q. Liu, C. Jin, Y. Ohishi and R. T. Oakley, *J. Am. Chem. Soc*., 2011, **133**, 6051; (c) K. Lekin, K. Ogata, A. Maclean, A. Mailman, S. M. Winter, A. Assoud, M. Mito, J. S. Tse, S. Desgreniers, N. Hirao, P. A. Dube and R. T. Oakley, *Chem. Commun.,* 2016, **52**, 13877.
[10] (a) S. M. Winter, S. Datta, S. Hill and R. T. Oakley, *J. Am. Chem. Soc.,* 2011, **133**, 8126; (b) S. M. Winter, R. T. Oakley, A. E. Kovalev and S. Hill, *Phys. Rev. B,* 2012, **85**, 094430; (c) K. Thirunavukkuarasu, S. M. Winter, C. C. Beedle, A. E. Kovalev, R. T. Oakley and S. Hill. *Phys. Rev. B*, 2015, **91**, 014412.
[11] (a) M. Deumal, M. A. Robb and J. J. Novoa, *Prog. Theor. Chem. Phys*., 2007, **16**, 271; (b) M. Deumal, S. LeRoux, J. M. Rawson, M. A. Robb and J. J. Novoa, *Polyhedron*, 2007, **26**, 1949; (c) J. J. Novoa, M. Deumal and J. Jornet-Somoza, *Chem. Soc. Rev*., 2011,**40**, 3182; (d) M. Fumanal, S. Vela, J. Ribas-Ariño and J. J. Novoa, *Chem. Asian J.,* 2014, **9**, 3612.
[12] (a) C. P. Constantinides, A. A. Berezin, G. A. Zissimou, M. Manoli, G. M. Leitus, M. Bendikov, M. R. Probert, J. M. Rawson and P. A. Koutentis, *J. Am. Chem. Soc*., **2014**, 136, 11906; (b) C. P. Constantinides, A. A. Berezin, M. Manoli, G. M. Leitus, G. A. Zissimou, M. Bendikov, J. M. Rawson and P. A. Koutentis, *Chem. Eur. J.* 2014, **20**, 5388; (c) C. P. Constantinides, D. B. Lawson, A. A. Berezin, G. A. Zissimou, M. Manoli, G. M. Leitus and P. A. Koutentis, *CrystEngComm*, 2019, **019**, 21, 4599.
[13] S. L. Veber, M. V. Fedin, A. I. Potapov, K. Y. Maryunina, G. V. Romanenko, R. Z. Sagdeev, V. I. Ovcharenko, D. Goldfarb and E. G. Bagryanskaya, *J. Am. Chem. Soc*., 2008, **130**, 2444.
[14] (a) M. R. Probert, C. M. Robertson, J. A. Coome, J. A. K. Howard, B. C. Michell and A. E. Goeta, *J. Appl. Cryst*., 2010, **43**, 1415. (b) J. A. K. Howard and M. R. Probert, *Science*, 2014, **343**, 1098.
[15] (a) A. Bondi, *J. Phys. Chem*., 1964, **68**, 441; (b) I. Dance, *New J. Chem*., 2003, **27**, 22.
[16] J. P. Malrieu, R. Caballol, C. J. Calzado, C. de Graaf and N. Guihéry, *Chem. Rev*., 2014, **114**, 429.
[17] J. H. Ammeter, H. B. Bürgi, J. C. Thibeault and R. Hoffmann, *J. Am. Chem. Soc.,* 1978, **100**, 3686.
[18] (a) L. Noodleman, *Chem. Phys*., 1981, **74**, 5737; (b) L. Noodleman and E. R. Davidson, *Chem. Phys*., 1986, **109**, 131; (c) H. Nagao, M. Nishino, Y. Shigeta, T. Soda, Y. Kitagawa, T. Onishi, Y. Yoshioka and K. Yamaguchi, *Coord. Chem. Rev*., 2000, **198**, 265.
[19] C. M. Robertson, A. A. Leitch, K. Cvrkalj, D. J. T. Myles, R. W. Reed, P. A. Dube and R. T. Oakley, *J. Am. Chem. Soc*., 2008, **130**, 14791.
[20] (a) M. Mito, Y. Komorida, H. Tsuruda, J. S. Tse, S. Desgreniers, Y. Ohishi, A. A. Leitch, K. Cvrkalj, C.M. Robertson and R. T. Oakley, *J. Am. Chem. Soc*., 2009, **131**, 16012; (b) K. Irie, K. Shibayama, M. Mito, S. Takagi, M. Ishizuka, K. Lekin and R. T. Oakley, *Phys. Rev. B,* 2019, **99**, 014417.
[21] A. D. Becke, *J. Chem. Phys*., 1993, **98**, 5648.
[22] C. Kittel, *Introduction to Solid State Physics*, 5th ed.; John Wiley& Sons: New York, 1996; p 462.
[23] N. Mardirossiana and M. Head-Gordon, *Molecular Phys*., 115, **19**, 2315.
[24] C. Adamo and V. Barone, *J. Chem. Phys*., 1999, **110**, 6158.
[25] É. Brémond, Á. J. Pérez-Jiménez, J. C. Sancho-García and C. Adamo, *J. Chem. Phys*., 2019, **150**, 201102.
[26] T. Yanai, D. P. Tew and N. C. Handy, *Chem. Phys. Lett*., 2004, **393**, 51.
[27] U. Salzner and A. Aydin, *J. Chem. Theory Comput*., 2011, **7**, 2568.
[28] M. A. Rohrdanz, K. M. Martins and J. M. Herbert, *J. Chem. Phys*., 2009, **130**, 054112.
[29] A. Jaoul, G. Nocton and C. Clavaguera, *ChemPhysChem,* 2017, **18**, 2688.
[30] (a) M. Fumanal and M. Deumal, *Phys. Chem. Chem. Phys.*, 2016, **18**, 20738. (b) M. Fumanal, J. Jornet-Somoza, S. Vela, J. J. Novoa, J. Ribas-Arino and M. Deumal, *J. Mater. Chem. C*, 2021, **9**, 10647.
[31] (a) A. Bencini and F. Totti, *J. Chem. Theory Comput.* 2009, **5**, 144; (b) A. C. Jacko and B. J. Powell, *Phys. Chem. Chem. Phys*., 2021, 23, 5012.
[32] A. Mailman, S. M. Winter, J. W. L. Wong, C. M. Robertson, A. Assoud, P. A. Dube and R. T. Oakley, *J. Am. Chem. Soc*., 2015, **137**, 1044.
[33] (a) M. Deumal, J. M. Rawson, A. E. Goeta, J. A. K. Howard, R. C. B. Copley, M. A. Robb and J. J. Novoa, *Chem. Euro. J*., 2010, **16**, 2741; (b) S. M. Winter, K. Cvrkalj, C. M. Robertson, M. R. Probert, P. A. Dube, J. A. K. Howard and R. T. Oakley, *Chem. Commun*., 2008, 7306; (c) C. Climent, S. Vela, J. Jornet-Somoza and M. Deumal, *Phys. Chem. Chem. Phys*., 2019, **21**, 12184.

